S_{E1} factor of radiative α capture on ^{12}C in cluster effective field theory

Shung-Ichi Ando*
School of Mechanical and ICT Convergence Engineering, Sunmoon University, Asan, Chungnam 31460, Republic of Korea

(Received 7 January 2019; published 26 July 2019)

The S_{E1} factor of radiative α capture on ^{12}C is studied in effective field theory up to next-to-leading order (NLO), and a modification of the counting rules for the radiative capture amplitudes is discussed. I find that only two unfixed parameters remain in the amplitudes up to NLO, and those two parameters are fitted to the experimental S_{E1} data. A value of the S_{E1} factor is calculated at the Gamow-peak energy as $S_{E1} = 59 \pm 3$ keV b, and the result is found to be about 30% smaller than the estimates reported recently. An uncertainty of the estimate in the present work is also discussed.

DOI: 10.1103/PhysRevC.100.015807

I. INTRODUCTION

The radiative α capture on carbon-12, $^{12}\mathrm{C}(\alpha,\gamma)^{16}\mathrm{O}$, is one of the fundamental reactions in nuclear astrophysics, which determines the C/O ratio created in the stars [1]. The reaction rate, equivalently the astrophysical S factor, of the process at the Gamow peak energy, $E_G = 0.3$ MeV, however, cannot be determined in experiment due to the Coulomb barrier. A theoretical model is necessary to be employed in order to extrapolate the reaction rate down to E_G by fitting model parameters to experimental data typically measured at a few MeV.

In constructing a model for the study, one needs to take account of excited states of ^{16}O [2], particularly, two excited bound states for $l^{\pi}_{i\mathrm{th}} = 1^-_1$ and 2^+_1 just below the α-^{12}C breakup threshold at $E = -0.045$ and -0.24 MeV,[1] respectively, as well as two resonant (second excited) 1^-_2 and 2^+_2 states at $E = 2.42$ and 2.68 MeV, respectively. The capture reaction to the ground state of ^{16}O at E_G is expected to be $E1$ and $E2$ transition dominant due to the subthreshold 1^-_1 and 2^+_1 states, while the resonant 1^-_2 and 2^+_2 states play a dominant role in the available experimental data at low energies, typically $1 \leqslant E \leqslant 3$ MeV. The main part of the S factor, therefore, consists of S_{E1} and S_{E2} from the $E1$ and $E2$ transitions along with a small contribution, S_{casc}, from so-called cascade transitions. During the last half century, a lot of experimental and theoretical studies for the reaction have been carried out. See Refs. [2–5] for review.

Theoretical frameworks employed for the study are mainly categorized into two [5]: the cluster models using generalized coordinate method [6] or potential model [7] and the phenomenological models using the parametrization of Breit-Wigner, R matrix [8], or K matrix [9]. A recent trend of the study is to rely on intensive numerical analysis, in which a larger amount of the experimental data relevant to the study are accumulated, and a significant number of parameters of the models are fitted to the data by using computational power [5,10,11]. In the present work, to the contrary, we discuss another approach to estimate the S factor at E_G; we employ a new method for the study and discuss a calculation of the S_{E1} factor at E_G based on an effective field theory.

Effective field theories (EFTs) provide us a model independent and systematic method for theoretical calculations. An EFT for a system in question can be built by introducing a scale which separates relevant degrees of freedom at low energies from irrelevant ones at high energies. An effective Lagrangian is written down in terms of the relevant degrees of freedom and perturbatively expanded by counting the number of derivatives order by order. The irrelevant degrees of freedom are integrated out, and their effect is embedded in coefficients appearing in the Lagrangian. Thus, a transition amplitude is systematically calculated by writing down Feynman diagrams, while the coefficients appearing in the Lagrangian are fixed by experiment. For review, one may refer to Refs. [12–15]. For last two decades, various processes essential in nuclear astrophysics have been investigated by constructing EFTs: $p(n,\gamma)d$ at big bang nucleosynthesis energies [16,17] and pp fusion [18–21],$^3\mathrm{He}(\alpha,\gamma)^7\mathrm{Be}$ [22,23], and $^7\mathrm{Be}(p,\gamma)^8\mathrm{B}$ [24,25] in the Sun.

In the previous works [26–28], I have constructed an EFT of the radiative capture reaction, $^{12}\mathrm{C}(\alpha,\gamma)^{16}\mathrm{O}$, derived the counting rules for the reaction at E_G, and fitted some parameters of the theory to the binding energies of the ground and excited states, 0^+_1, 0^+_2, 1^-_1, 2^+_1, and 3^-_1 ($l^{\pi}_{i\mathrm{th}}$) states of ^{16}O and the phase shift data of the elastic α-^{12}C scattering for $l = 0, 1, 2$, and 3 channels. (The counting rules for the radiative capture reaction are reviewed in the following sections.) When fitting the parameters to the phase shift data, I have introduced resonance energies of ^{16}O as a large scale of the theory. As suggested by Teichmann [29], below the resonance energies, the Breit-Wigner-type parametrization for resonances can be expanded in powers of the energy, and one obtains an expression of the elastic scattering amplitude as the effective range expansion. In addition, I have included the effective range parameters up to third order ($n = 3$ in powers

*sando@sunmoon.ac.kr

[1]The energy E denotes that of the α-^{12}C system in the center of mass frame.

of k^{2n}) for the $l = 0, 1, 2$ channels and up to fourth order ($n = 4$) for the $l = 3$ channel because of the modification of the counting rules discussed in Ref. [27]. Though the phase shift data below the resonance energies are reproduced very well by using the fitted parameters, I find that significant uncertainties in the elastic scattering amplitudes remain when interpolating them to E_G.

In the present work, I apply the calculation method of EFT to the study of the S_{E1}-factor of the radiative capture process up to next-to-leading order (NLO). Inclusion of the photon field into the present formalism is straightforward because a photon field abides in covariant derivatives in the terms of the effective Lagrangian. In the standard counting rules, one approximately has three structures (momentum dependence) in the radiative capture amplitudes after fitting the effective range parameters to the phase shift data of the elastic scattering for $l = 1$. I discuss a modification of the standard counting rules because of an enhancement effect of the p-wave composite ^{16}O propagator. After taking the modification into account, one has two structures, which are represented by two unknown constants, in the radiative capture amplitudes. The two constants are fitted to the experimental S_{E1} data, and I calculate an S_{E1} factor at E_G. I find that the result is about 30% smaller than the other estimates reported recently, and then discuss an uncertainty of the result of the present work from higher order terms of the theory.

The present paper is organized as follows. In Sec. II, the counting rules of EFT and the effective Lagrangian for the reactions are briefly reviewed, and the radiative capture amplitudes for the initial p-wave state and the formula of the S_{E1} factor are displayed in Sec. III. In Sec. IV, a modification of the counting rules is discussed, and numerical results are presented in Sec. V. Finally, in Sec. VI, results and discussion of the present work are presented.

II. EFFECTIVE LAGRANGIAN

In the study of the radiative capture process, $^{12}\mathrm{C}(\alpha,\gamma)^{16}\mathrm{O}$, at $E_G = 0.3\,\mathrm{MeV}$ employing an EFT, one may regard the ground states of α and ^{12}C as point-like particles whereas the first excited states of α and ^{12}C are chosen as irrelevant degrees of freedom, from which a large scale of the theory is determined [26]. Thus the expansion parameter of the theory is $Q/\Lambda_H \approx 1/3$, where Q denotes a typical momentum scale $Q \approx k_G$; k_G is the Gamow peak momentum, $k_G = \sqrt{2\mu E_G} \simeq 41\,\mathrm{MeV}$, where μ is the reduced mass of α and ^{12}C. Λ_H denotes a large momentum scale $\Lambda_H \simeq \sqrt{2\mu_4 E_{(4)}}$ or $\sqrt{2\mu_{12}E_{(12)}} \approx 150\,\mathrm{MeV}$ where μ_4 is the reduced mass of one and three-nucleon system and μ_{12} is that of four and eight-nucleon system. $E_{(4)}$ and $E_{(12)}$ are the first excited energies of α and ^{12}C, respectively. By including terms up to next-to-next-to-leading order, for example, one may have about 10% theoretical uncertainty for the amplitude.

The inclusion of the ground state of ^{16}O, one may think, could cause a problem because the binding energy of ^{16}O from the α and ^{12}C breakup threshold is $B_0 = 7.162\,\mathrm{MeV}$, which is larger than the energy of the first excited (2^+_1) state of ^{12}C, $E_{(12)} = 4.440\,\mathrm{MeV}$. However, almost all of the energy released through the capture reaction is carried away by the outgoing photon, and thus the initial and final nuclear states remain in the states at the typical energies. After the photon is emitted, the large momentum scale appears in the intermediate state in the α-^{12}C propagation, but because the binding energy is far below the α-^{12}C threshold, its physical effect to the α-^{12}C propagation is small. In the present work, I do not introduce the ^{16}O ground state as a dynamical degree of freedom but a source field because the ^{16}O ground state appears only in the final state.

An effective Lagrangian for the study of the radiative capture reaction may be written as [26,30–33]

$$\begin{aligned}\mathcal{L} =& \phi_\alpha^\dagger\left(iD_0 + \frac{\vec{D}^2}{2m_\alpha} + \cdots\right)\phi_\alpha + \phi_C^\dagger\left(iD_0 + \frac{\vec{D}^2}{2m_C} + \cdots\right)\phi_C \\ &+ \sum_{n=0}^{3} C_n^{(1)} d_i^\dagger\left[iD_0 + \frac{\vec{D}^2}{2(m_\alpha + m_C)}\right]^n d_i \\ &- y^{(1)}\left[d_i^\dagger\left(\phi_\alpha O_i^{(1)}\phi_C\right) + \left(\phi_\alpha O_i^{(1)}\phi_C\right)^\dagger d_i\right] \\ &- y^{(0)}[\phi_O^\dagger(\phi_\alpha\phi_C) + (\phi_\alpha\phi_C)^\dagger\phi_O] \\ &- h^{(1)}\frac{y^{(0)}y^{(1)}}{\mu}\left[\left(\mathcal{O}_i^{(1)}\phi_O\right)^\dagger d_i + \mathrm{H.c.}\right] + \cdots, \end{aligned} \tag{1}$$

where ϕ_α (m_α) and ϕ_C (m_C) are fields (masses) of α and ^{12}C, respectively. ϕ_O ($\phi_O^\dagger$) is introduced as a source field for the ^{16}O ground state in the final (initial) state. In the second last term in Eq. (1), for example, ϕ_O ($\phi_O^\dagger$) destroys (creates) the ^{16}O ground state, and $(\phi_\alpha\phi_C)^\dagger$ [$(\phi_\alpha\phi_C)$] fields create (destroy) an s-wave α-^{12}C state. The transition rate between the ^{16}O ground state and the s-wave α-^{12}C state is parametrized in terms of the coupling constant $y^{(0)}$, which is fixed by using experimental data. D^μ is a covariant derivative, $D^\mu = \partial^\mu + i\mathcal{Q}A^\mu$, where $\mathcal{Q}$ is a charge operator and A^μ is the photon field. The dots denote higher order terms. d_i is a composite field of ^{16}O consisting of α and ^{12}C fields for $l = 1$ channel. The operators for the $l = 1$ channel are given as

$$O_l^{(1)} = i\left(\frac{\overrightarrow{D}_C}{m_C} - \frac{\overleftarrow{D}_\alpha}{m_\alpha}\right)_i, \quad \mathcal{O}_i^{(1)} = \frac{iD_i}{m_O}, \tag{2}$$

where m_O is the mass of ^{16}O in ground state. The coupling constants, $C_n^{(1)}$ with $n = 0, 1, 2$, and 3, are fixed by using the effective range parameters of elastic α-^{12}C scattering for $l = 1$, while the coupling constant $y^{(1)}$ is redundant; I set it as $y^{(1)} = \sqrt{6\pi\mu}$.[2] A contact interaction, the $h^{(1)}$ term, is introduced to renormalize divergence from loop diagrams.

III. AMPLITUDES AND THE S_{E1} FACTOR

In Fig. 1, diagrams for dressed composite propagators of ^{16}O consisting of α and ^{12}C for $l = 1$ are depicted, in which

[2]In the denominator of the elastic scattering amplitude, the couplings appear in the form, $C_n^{(1)}/y^{(1)2}$ with $n = 0, 1, 2, 3$, and are fitted to the effective range parameters, $1/a_1$, r_1, P_1, Q_1, for $l = 1$, respectively. The $y^{(1)}$ coupling is redundant, and one can arbitrarily fix its value.

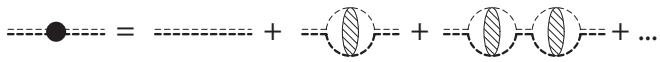

FIG. 1. Diagrams for dressed ^{16}O propagators. A thick (thin) dashed line represents a propagator of ^{12}C (α), and a thick and thin double dashed line with and without a filled circle represent a dressed and bare ^{16}O propagator, respectively. A shaded oval represents a set of diagrams consisting of all possible one-potential-photon-exchange diagrams up to infinite order and no potential-photon-exchange one.

the Coulomb interaction between α and ^{12}C is taken into account [26,27]. In Fig. 2, diagrams of the radiative capture process from the initial $l = 1$ state to the ^{16}O ground (0^+_1) state are depicted, in which the Coulomb interaction between α and ^{12}C is taken into account as well.

The radiative capture amplitude for the initial $l = 1$ state is presented as

$$A^{(l=1)} = \vec{\epsilon}^{\,*}_{(\gamma)} \cdot \hat{p} X^{(l=1)}, \tag{3}$$

where $\vec{\epsilon}^{\,*}_{(\gamma)}$ is the polarization vector of outgoing photon and $\hat{p} = \vec{p}/|\vec{p}|$; $\vec{p}$ is the relative momentum of the initial α and ^{12}C. The amplitude $X^{(l=1)}$ can be decomposed as

$$X^{(l=1)} = X^{(l=1)}_{(a+b)} + X^{(l=1)}_{(c)} + X^{(l=1)}_{(d+e)} + X^{(l=1)}_{(f)}, \tag{4}$$

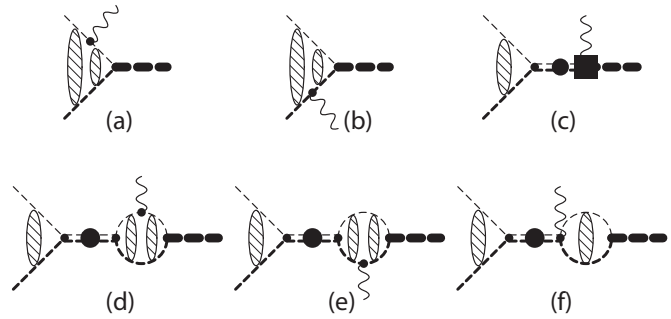

FIG. 2. Diagrams for the radiative capture process from the initial p-wave α-^{12}C state. A wavy line denotes the outgoing photon, a thick and thin double dashed line with a filled circle in the intermediate state, whose diagrams are displayed in Fig. 1, the dressed composite ^{16}O propagator for $l = 1$, and a thick dashed line in the final state the ground (0^+_1) state of ^{16}O. See the caption of Fig. 1 as well.

where those amplitudes correspond to the diagrams depicted in Fig. 2.

I follow the calculation method suggested by Ryberg *et al.* [34], in which Coulomb Green's functions are represented in coordinate space satisfying appropriate boundary conditions. Thus I obtain the expression of those amplitudes in center of mass frame as

$$X^{(l=1)}_{(a+b)} = 2y^{(0)} e^{i\sigma_1} \Gamma(1+\kappa/\gamma_0) \int_0^\infty dr r W_{-\kappa/\gamma_0,\frac{1}{2}}(2\gamma_0 r) \left[\frac{Z_\alpha \mu}{m_\alpha} j_0\left(\frac{\mu}{m_\alpha} k' r\right) - \frac{Z_C \mu}{m_C} j_0\left(\frac{\mu}{m_C} k' r\right) \right] \left\{ \frac{\partial}{\partial r}\left[\frac{F_1(\eta, pr)}{pr}\right] + 2\frac{F_1(\eta, pr)}{pr^2} \right\}, \tag{5}$$

$$X^{(l=1)}_{(c)} = +y^{(0)} h^{(1)R} \frac{6\pi Z_O}{\mu m_O} \frac{e^{i\sigma_1} p\sqrt{1+\eta^2} C_\eta}{K_1(p) - 2\kappa H_1(p)}, \tag{6}$$

$$X^{(l=1)}_{(d+e)} = +i\frac{2}{3} y^{(0)} \frac{e^{i\sigma_1} p^2 \sqrt{1+\eta^2} C_\eta}{K_1(p) - 2\kappa H_1(p)} \Gamma(1+\kappa/\gamma_0)\Gamma(2+i\eta) \int_{r_C}^\infty dr r W_{-\kappa/\gamma_0,\frac{1}{2}}(2\gamma_0 r) \left[\frac{Z_\alpha \mu}{m_\alpha} j_0\left(\frac{\mu}{m_\alpha} k' r\right) - \frac{Z_C \mu}{m_C} j_0\left(\frac{\mu}{m_C} k' r\right) \right]$$
$$\times \left\{ \frac{\partial}{\partial r}\left[\frac{W_{-i\eta,\frac{3}{2}}(-2ipr)}{r}\right] + 2\frac{W_{-i\eta,\frac{3}{2}}(-2ipr)}{r^2} \right\}, \tag{7}$$

$$X^{(l=1)}_{(f)} = -3y^{(0)} \mu [-2\kappa H(\eta_{b0})] \left(\frac{Z_\alpha}{m_\alpha} - \frac{Z_C}{m_C} \right) \frac{e^{i\sigma_1} p\sqrt{1+\eta^2} C_\eta}{K_1(p) - 2\kappa H_1(p)}, \tag{8}$$

where k' is the magnitude of outgoing photon momentum, and κ is the inverse of the Bohr radius, $\kappa = Z_\alpha Z_C \mu \alpha_E$, where α_E is the fine structure constant. Z_α, Z_C, and Z_O are the number of protons in α, ^{12}C and ^{16}O, respectively. η is the Sommerfeld parameter, $\eta = \kappa/p$, and γ_0 is the binding momentum of the ground state of ^{16}O, $\gamma_0 = \sqrt{2\mu B_0}$. $\Gamma(z)$ and $j_l(x)$ are the gamma function and spherical Bessel function, respectively, while $F_l(\eta, \rho)$ and $W_{k,\mu}(z)$ are regular Coulomb function and Whittaker function, respectively. In addition,

$$e^{i\sigma_1} = \sqrt{\frac{\Gamma(2+i\eta)}{\Gamma(2-i\eta)}}, \quad C_\eta^2 = \frac{2\pi\eta}{e^{2\pi\eta} - 1},$$
$$H_1(p) = p^2(1+\eta^2) H(\eta) \tag{9}$$

with

$$H(\eta) = \psi(i\eta) + \frac{1}{2i\eta} - \ln(i\eta), \tag{10}$$

where $\psi(z)$ is digamma function.

The function $K_1(p)$ contains the information about nuclear interaction and is represented in terms of the effective range parameters of the elastic α-^{12}C scattering for $l = 1$ as[3]

$$K_1(p) = -\frac{1}{a_1} + \frac{1}{2} r_1 p^2 - \frac{1}{4} P_1 p^4 + Q_1 p^6, \tag{11}$$

[3]In the previous work, I had used another parametrization, the so-called v parameterization, to represent the effective range parameters [35].

where a_1 is fixed by using the binding energy of the 1^-_1 bound state of ^{16}O, and other effective range parameters, r_1, P_1, and Q_1, are fitted to the experimental phase shift data.

Regarding the divergence from the loop diagrams, the loops of the diagrams (a) and (b) in Fig. 2 are finite, while those of the diagrams (d) and (e) lead to a log divergence in $X^{(l=1)}_{(d+e)}$ in the limit, $r \to 0$. I introduce a short range cutoff r_C in the r integral in Eq. (7), and the divergence is renormalized by the counter term, $h^{(1)}$. The loop of the diagram (f) diverges and is renormalized by the $h^{(1)}$ term as well. Thus I obtain

$$h^{(1)R} = h^{(1)} - \mu \frac{m_O}{Z_O}\left(\frac{Z_\alpha}{m_\alpha} - \frac{Z_C}{m_C}\right)\left[I^{\rm div}_{(d+e)} + J^{\rm div}_0\right], \quad (12)$$

where $I^{\rm div}_{(d+e)}$ is the divergence term from the diagrams (d) and (e) and $J^{\rm div}_0$ is that from the diagram (f); I obtain

$$I^{\rm div}_{(d+e)} = -\frac{\kappa\mu}{9\pi}\int_0^{r_C}\frac{dr}{r},$$
$$J^{\rm div}_0 = \frac{\kappa\mu}{2\pi}\left[\frac{1}{\epsilon} - 3C_E + 2 + \ln\left(\frac{\pi\mu^2_{DR}}{4\kappa^2}\right)\right], \quad (13)$$

where, to derive the expression of $J^{\rm div}_0$, the dimensional regularization in $4-2\epsilon$ space-time dimensions has been used; $C_E = 0.577\ldots$ and μ_{DR} is a scale factor from the dimensional regularization. $h^{(1)R}$ is a renormalized coupling constant which is fixed by experiment.

From the loop diagram (f), when the Coulomb interaction is ignored, the large momentum scale $\gamma_0 \simeq 200$ MeV is picked up in the numerator of the amplitude. It causes the emergence of a term which does not obey the counting rules.[4] In the present case, the large momentum scale γ_0 from the ground state energy of ^{16}O appears as a ratio κ/γ_0, due to the nonperturbative Coulomb interaction, where κ is another large momentum scale, $\kappa \simeq 245$ MeV. The finite term $-2\kappa H(\eta_{b0})$ in $X^{(l=1)}_{(f)}$ from the loop of the diagram (f) where $\eta_{b0} = \kappa/(i\gamma_0)$ is reduced to a typical momentum scale, $-2\kappa H(\eta_{b0}) = 25.8$ MeV.

The S_{E1} factor is defined by

$$S_{E1}(E) = \sigma_{E1}(E) E e^{2\pi\eta}, \quad (14)$$

where the total cross section is

$$\sigma_{E1}(E) = \frac{4}{3}\frac{\alpha_E \mu E'_\gamma}{p(1+E'_\gamma/m_O)}|X^{(l=1)}|^2 \quad (15)$$

with

$$E'_\gamma \simeq B_0 + E - \frac{1}{2m_O}(B_0+E)^2. \quad (16)$$

[4]A method to renormalize a term which does not obey counting rules in an EFT (manifestly Lorentz invariant baryon chiral perturbation theory) is known as the extended on mass shell (EOMS) scheme [36,37]; one can renormalize the term proportional to γ_0 in the counter term, $h^{(1)R}$, even when the Coulomb interaction is ignored.

IV. MODIFICATION OF THE COUNTING RULES

Before fitting the parameters to available experimental data, I discuss a modification of the standard counting rules for the radiative capture amplitudes. An order of an amplitude from each of the diagrams is found by counting the number of momenta of vertices and propagators in a Feynman diagram. Thus one has a leading order (LO) amplitude from the diagram (c), because the contact γ-d_i-ϕ_O vertex of the $h^{(1)R}$ term does not have a momentum dependence, and NLO amplitudes from the other diagrams in Fig. 2. One may notice a large suppression factor, $Z_\alpha/m_\alpha - Z_C/m_C$, appearing in $X^{(l=1)}_{(f)}$; $(m_O/Z_O)(Z_\alpha/m_\alpha - Z_C/m_C) \simeq -6.5\times10^{-4}$. Similar suppression effect can be found in $X^{(l=1)}_{(a+b)}$ and $X^{(l=1)}_{(d+e)}$ as well; I denote those amplitudes as X^-, and when changing the minus sign to the plus one in the front of the spherical Bessel function $j_0(z)$ in Eqs. (5) and (7), I do them as X^+. I thus find $|X^{(l=1)-}_{(a+b)}/X^{(l=1)+}_{(a+b)}| \simeq 8.7\times10^{-4}$ and $|X^{(l=1)-}_{(d+e)}/X^{(l=1)+}_{(d+e)}| \simeq 3.6\times10^{-4}$ at the energy range, $E = 0.9 - 3$ MeV, at which I fit the parameters to the experimental S_{E1} data in the next section. The suppression effect is common among those amplitudes, thus it does not alter the order counting of the diagrams.

The strong suppression effect mentioned above is well known; the $E1$ transition is strongly suppressed between isospin-zero ($N = Z$) nuclei. This mechanism is recently reviewed and studied for $\alpha(d,\gamma)^6$Li reaction by Baye and Tursunov [38]. In the standard microscopic calculations with the long-wavelength approximation, the term proportional to $Z_1/m_1 - Z_2/m_2$ vanishes because of the standard choice of mass of nuclei as $m_i = A_i m_N$ where A_i is the mass number of ith nucleus and m_N is the nucleon mass. I have strongly suppressed but nonzero contribution above because of the use of the physical masses for α and ^{12}C. The small but nonvanishing $E1$ transition for the $N = Z$ cases has intensively been studied in the microscopic calculations and can be accounted by two effects: one is the second order term of the $E1$ multipole operator in the long-wavelength approximation [39], and the other is due to the mixture of the small $T = 1$ configuration in the actual nuclei [40]. In the present approach, the first one may be difficult to incorporate for the point-like particles while the second one could be introduced from a contribution at high energy: At $E \simeq 5$ MeV and 8.5 MeV above the α-^{12}C breakup threshold, p-^{15}N and n-^{15}O breakup channels, respectively, are open, and $T = 1$ resonant states of ^{16}O start emerging (along with the $T = 1$ isobars, ^{16}N, ^{16}O, and ^{16}F). I might have introduced the p-^{15}N and n-^{15}O fields as relevant degrees of freedom in the theory. The p-^{15}N and n-^{15}O fields, then, appear in the intermediate states, as p-^{15}N or n-^{15}O propagation, in the loop diagrams (d), (e), (f) in Fig. 2 instead of the α-^{12}C propagation. One may introduce a mixture of the isospin $T = 0$ and $T = 1$ states in the p-^{15}N or n-^{15}O propagation, and the strong $E1$ suppression is circumvented in the loops. (The contribution from the p-^{15}N and n-^{15}O channels for the ^{12}C$(\alpha,\gamma)^{16}$O reaction has already been studied in the microscopic approach [41].) In the present work, however, the p-^{14}N and n-^{15}O fields are regarded as irrelevant degrees of freedom at the high energy and integrated out of the effective Lagrangian. Its effect, thus, is embedded in

the coefficient of the contact interaction, the $h^{(1)R}$ term, in the (c) diagram while the $h^{(1)R}$ term is fitted to the experimental S_{E1} data in the next section.

I now discuss an enhancement effect which modifies the counting rules for the amplitudes due to the p-wave dressed ^{16}O propagator in the diagrams (c), (d), (e), and (f). The p-wave dressed ^{16}O propagator is enhanced due to large cancellations between the effective range terms and terms generated from the Coulomb self-energy term $H_1(p)$, as discussed in Ref. [27]. In the standard counting rules, the order of the propagator is assigned to Q^{-3}, while because of the inclusion up to the $Q_1 p^6$ term in the effective range expansion it should be counted as Q^{-7}. Thus the enhancement factor will be $(Q/\Lambda_H)^{-4} \approx 100$. To check the magnitude of the enhancement effect, I calculate a ratio of the amplitudes and have $|(X^{(l=1)}_{(c)} + X^{(l=1)}_{(d+e)} + X^{(l=1)}_{(f)})/X^{(l=1)}_{(a+b)}| \approx 380 - 30$ at $E = 0.1$–3 MeV after fixing $h^{(1)R}$ to the S_{E1} data. (Here, we have used a value of $h^{(1)R}$ at $r_C = 0.1$ fm.) One can see that the nonpole amplitude $X^{(l=1)}_{(a+b)}$ is significantly suppressed compared to the other amplitudes (while one may notice that the counting rules are applicable at $E_G = 0.3$ MeV).

V. NUMERICAL RESULTS

Five parameters to fit to the data remain in the radiative capture amplitudes; three parameters, r_1, P_1, Q_1, are fitted to phase shift data of the elastic scattering and the other two parameters, $h^{(1)R}$ and $y^{(0)}$, are to the experimental S_{E1} data. The standard χ^2 fit is performed by employing a Markov chain Monte Carlo method for the parameter fitting.[5] The phase shift data for $l = 1$ are taken from Tischhauser *et al.*'s paper [43], and the experimental S_{E1} data are from the literature summarized in Tables V and VII in Ref. [5]: Dyer and Barnes (1974) [44], Redder *et al.* (1987) [45], Ouellet *et al.* (1996) [46], Roters *et al.* (1999) [47], Gialanella *et al.* (2001) [48], Kunz *et al.* (2001) [49], Fey (2004) [50], Makii *et al.* (2009) [51], and Plag *et al.* (2012) [52].

I fit the effective range parameters to the phase shift data for $l = 1$ at $E_\alpha = 2.6$–6.0 MeV and have

$$r_1 = 0.415272(9)\,\mathrm{fm}^{-1}, \quad P_1 = -0.57473(9)\ \mathrm{fm}, \\ Q_1 = 0.02018(3)\ \mathrm{fm}^3, \tag{17}$$

where the number of the data is $N = 273$ and $\chi^2/N = 0.74$. The uncertainties of the fitted values stem from those of the experimental data. The scattering volume a_1 is fixed by using the condition that the denominator of the elastic scattering amplitude vanishes at the binding energy of the 1^-_1 state, $E = -0.045$ MeV. Using the relation in Eq. (6) in Ref. [27] and the values of the fitted effective range parameters, one has

$$a_1 = -1.658 \times 10^5\,\mathrm{fm}^3. \tag{18}$$

In Fig. 3, a curve of the phase shift δ_1 calculated by using the fitted effective range parameters is plotted as a function of E_α, where E_α is the α energy in laboratory frame.[6] The

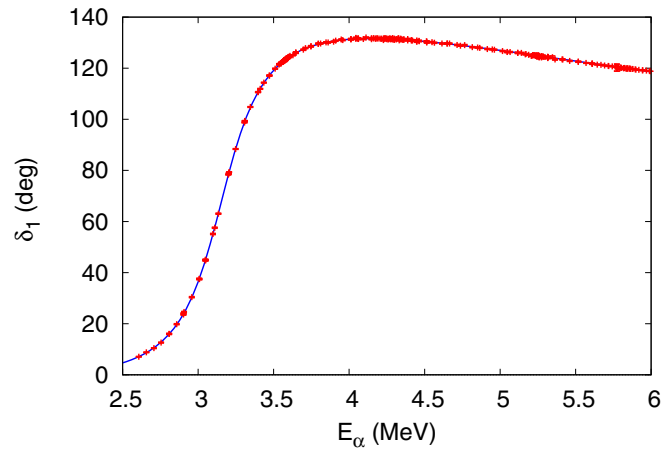

FIG. 3. Phase shift, δ_1, plotted by using the fitted effective range parameters, r_1, P_1, Q_1 as a function of E_α. The experimental phase shift data are also displayed in the figure.

experimental data are displayed in the figure as well. One can see that the theory curve well reproduces the experimental data at the energy range, $E_\alpha = 2.6$–6.0 MeV. Because the energy range is over the energy of 1^-_2 state, $E = 2.43$ MeV ($E_\alpha = 3.23$ MeV) and below that of 1^-_3 state, $E = 5.29$ MeV ($E_\alpha = 7.05$ MeV), the result indicates that the expression of the effective range expansion given in Eq. (11) is reliable to describe the 1^-_1 and 1^-_2 states up to $E_\alpha = 6.0$ MeV.

I fit the parameters, $h^{(1)R}$ and $y^{(0)}$, to the experimental data of S_{E1} at the energy range, $E = 0.9$–3.0 MeV using some values of the cutoff r_C in the range, $r_C = 0.01$–0.35 fm, in the r integral in $X^{(l=1)}_{(d+e)}$ in Eq. (7). The number of the data is $N = 151$. In Table I, fitted values of $h^{(1)R}$ and $y^{(0)}$ along with χ^2/d.o.f and estimates of S_{E1} at E_G are displayed. The uncertainties of the fitted values of $h^{(1)R}$ and $y^{(0)}$ stem from those of the experimental data. One finds a significant cutoff dependence of the couplings, $h^{(1)R}$ and $y^{(0)}$, and the S_{E1} factor at E_G in the table when varying the short range cutoff, $r_C = 0.01$–0.35 fm; as the values of r_C become larger, the χ^2/d.o.f. become larger while the S_{E1} values become smaller. One may also see that the variation of the S_{E1} factor becomes stable at the cutoff values smaller than $r_C = 0.1$ fm where the χ^2/d.o.f remain in stable and smaller values. In Fig. 4, a curve of S_{E1}

TABLE I. Fitted values of the coupling constants, $h^{(1)R}$ and $y^{(0)}$, to experimental data of S_{E1} at $E = 0.9$–3 MeV with the cutoff $r_C = 0.01$–0.35 fm. The number of the data is $N = 151$. The values in the fourth column are χ^2/d.o.f. of the fittings, and those in the last column are our results of S_{E1} at $E_G = 0.3$ MeV.

r_C (fm)	$h^{(1)R}\times 10^4$ (MeV^3)	$y^{(0)}$ (MeV$^{-1/2}$)	χ^2/d.o.f	S_{E1} (keV b)
0.01	5.2684(11)	0.253(9)	1.691	60.3(18)
0.035	2.4483(11)	0.310(11)	1.697	59.8(18)
0.05	1.5294(11)	0.347(12)	1.700	59.3(18)
0.1	−0.0695(11)	0.495(18)	1.715	57.9(17)
0.2	−1.1909(11)	0.943(34)	1.763	53.6(15)
0.35	−1.7106(12)	2.249(84)	1.926	42.1(10)

[5]I employ a PYTHON package, EMCEE [42], for the fitting.

[6]The center of mass energy E is related to E_α by $E_\alpha \simeq \frac{4}{3}E$.

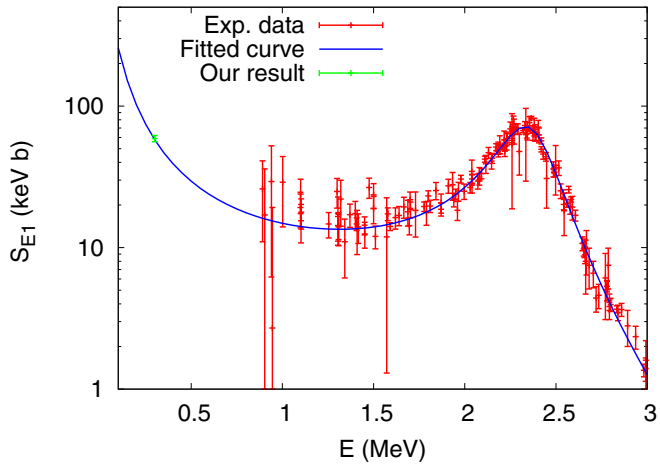

FIG. 4. S_{E1} factor plotted by using the fitted parameters with $r_C = 0.1$ fm as a function of E. The experimental data and our estimate of S_{E1} at E_G are also displayed in the figure.

calculated by using the fitted parameters at $r_C = 0.1$ fm is plotted. The experimental data and the result of S_{E1} at E_G to be mentioned below are displayed in the figure as well. One can see that the theory curve reproduces well the experimental data.

In the present work, I choose the results of S_{E1} with χ^2/d.o.f $\simeq 1.7$, in the cutoff region of the stability of S_{E1}, for our estimate of S_{E1} at the Gamow-peak energy, $E_G = 0.3$ MeV, thus, I have

$$S_{E1} = 59 \pm 3 \text{ keV b}, \tag{19}$$

where the small, about 5%, uncertainty stems from those of $h^{(1)R}$ and $y^{(0)}$ in Table I as well as that of the r_C dependence of S_{E1} within χ^2/d.o.f. $\simeq 1.7$. The previous estimates of the S_{E1} factor at E_G are well summarized in Table IV in Ref. [5]. The reported values are scattered from 1 to 340 keV b with various size of the error bars. Nonetheless it is worth pointing out that the result of the present work is about 30% smaller than those reported recently: 86 ± 22 by Tang *et al.* (2010) [53], 83.4 by Schurmann *et al.* (2012) [54], 100 ± 28 by Oulebsir *et al.* (2012) [55], 80 ± 18 by Xu *et al.* (2013) [10], 98.0 ± 7.0 by An *et al.* (2015) [11], and 86.3 by deBoer *et al.* (2017) [5].

Regarding the theoretical uncertainty of the present calculation, as discussed above, the nonpole amplitude $X^{(l=1)}_{(a+b)}$ is suppressed and gives less than one percent correction to S_{E1} at E_G. In the other amplitudes, $X^{(l=1)}_{(c)}$, $X^{(l=1)}_{(d+e)}$, and $X^{(l=1)}_{(f)}$, I find that $X^{(l=1)}_{(d+e)}$ and $X^{(l=1)}_{(c+f)} (= X^{(l=1)}_{(c)} + X^{(l=1)}_{(f)})$ have different momentum dependence and are considerably canceled with each other. I obtain $|(X^{(l=1)}_{(c+f)} + X^{(l=1)}_{(d+e)})/X^{(l=1)}_{(c+f)}| = 0.055$–$0.023$ at $E = 0.1$–3 MeV; the result is almost linearly decreasing as a function of $E = p^2/(2\mu)$. It implies that a higher order correction at N^{3}LO effectively exists in $X^{(l=1)}_{(d+e)}$ while those two contributions, $X^{(l=1)}_{(c+f)}$ and $X^{l=1)}_{(d+e)}$, at LO + NLO and N^{3}LO equally play a significant role to reproduce the S_{E1} data. Though I have not studied a complete set of the corrections at N^{3}LO, a next higher order correction appears at N^{5}LO (because a momentum $\vec{p}$ is vector, but a correction should be scalar, p^2). Thus the higher order correction at N^{5}LO which I do not have in the present work may give a few percent correction, $(Q/\Lambda_H)^4 \simeq 0.012$, to the estimate of S_{E1} at E_G.

VI. RESULTS AND DISCUSSION

In this work, I have applied a framework of EFT to the study of radiative α capture on ^{12}C for the first time. I have derived the radiative capture amplitudes up to NLO in the standard counting rules, and discussed a modification of the counting rules for the radiative capture amplitudes because of the enhancement of the p-wave dressed composite propagator of ^{16}O. I find that the nonpole amplitude $X^{(l=1)}_{(a+b)}$ is significantly suppressed in the present study. After taking the modification into account, approximately two independent structures (momentum dependence) remain in the amplitudes, $X^{(l=1)}_{(c+f)}$ and $X^{(l=1)}_{(d+e)}$. I also find that two unknown parameters remain in the amplitudes. The two parameters are fitted to the experimental S_{E1} data at $E = 0.9$–3.0 MeV, and I find the S_{E1} factor, $S_{E1} = 59 \pm 3$ keV b at E_G. The result of S_{E1} at E_G is about 30% smaller than the recent estimates, though I have not examined a convergence of the result yet.

A unique feature of EFT is that one can control a theoretical uncertainty of a physical quantity in theory. In the present work, however, I do not examine a convergence of the perturbative expansion of the amplitudes in the estimate of the S_{E1} factor because I did not include a complete set of the higher order corrections. Thus to study higher order corrections to the radiative capture amplitude up to the Q^4 order is important in order to check the convergence of the expansion series and estimate a theoretical uncertainty of S_{E1} at E_G. Nonetheless, to accurately fix additional parameters, when one includes higher order terms, may not be straightforward due to the present quality of the experimental data set of S_{E1}. It might be better studying the other quantities at low energies, such as the β-delayed α emission spectrum of ^{16}N or the γ angular distribution of the radiative α capture process by employing the present EFT approach.

ACKNOWLEDGMENTS

The author would like to thank Kyungsik Kim, Young-Ho Song, Youngman Kim, and Renato Higa for useful discussions. This work was supported by the Basic Science Research Program through the National Research Foundation of Korea funded by the Ministry of Education of Korea (Grant No. NRF-2016R1D1A1B03930122) and in part by the National Research Foundation of Korea (NRF) grant funded by the Korean government (Grants No. NRF-2013M7A1A1075764 and No. NRF-2016K1A3A7A09005580).

[1] W. A. Fowler, Rev. Mod. Phys. **56**, 149 (1984).
[2] L. R. Buchmann and C. A. Barnes, Nucl. Phys. A **777**, 254 (2006).
[3] A. Coc, F. Hammache, and J. Kiener, Eur. Phys. J. A **51**, 34 (2015).
[4] C. A. Bertulani and T. Kajino, Prog. Part. Nucl. Phys. **89**, 56 (2016).
[5] R. J. deBoer *et al.*, Rev. Mod. Phys. **89**, 035007 (2017), and references therein.
[6] P. Descouvemont, D. Baye, and P.-H. Heenen, Nucl. Phys. A **430**, 426 (1984).
[7] K. Langanke and S. E. Koonin, Nucl. Phys. A **439**, 384 (1985).
[8] A. M. Lane and R. G. Thomas, Rev. Mod. Phys. **30**, 257 (1958).
[9] J. Humblet, P. Dyer, and B. A. Zimmerman, Nucl. Phys. A **271**, 210 (1976).
[10] Y. Xu *et al.*, Nucl. Phys. A **918**, 61 (2013).
[11] Z.-D. An *et al.*, Phys. Rev. C **92**, 045802 (2015).
[12] P. F. Bedaque and U. van Kolck, Annu. Rev. Nucl. Part. Sci. **52**, 339 (2002).
[13] E. Braaten and H.-W. Hammer, Phys. Rep. **428**, 259 (2006).
[14] U.-G. Meißner, Phys. Scr. **91**, 033005 (2016).
[15] H.-W. Hammer, C. Ji, and D. R. Phillips, J. Phys. G **44**, 103002 (2017).
[16] G. Rupak, Nucl. Phys. A **678**, 405 (2000).
[17] S. Ando, R. H. Cyburt, S. W. Hong, and C. H. Hyun, Phys. Rev. C **74**, 025809 (2006).
[18] X. Kong and F. Ravndal, Nucl. Phys. A **656**, 421 (1999).
[19] M. Butler and J.-W. Chen, Phys. Lett. B **520**, 87 (2001).
[20] S. Ando, J. W. Shin, C. H. Hyun, S. W. Hong, and K. Kubodera, Phys. Lett. B **668**, 187 (2008).
[21] J.-W. Chen, C.-P. Liu, and S.-H. Yu, Phys. Lett. B **720**, 385 (2013).
[22] R. Higa, G. Rupak, and A. Vaghani, Eur. Phys. J. A **54**, 89 (2018).
[23] X. Zhang, K. M. Nollett, and D. R. Phillips, arXiv:1811.07611.
[24] X. Zhang, K. M. Nollett, and D. R. Phillips, Phys. Rev. C **89**, 051602(R) (2014).
[25] E. Ryberg, C. Forssén, H.-W. Hammer, and L. Platter, Eur. Phys. J. A **50**, 170 (2014).
[26] S.-I. Ando, Eur. Phys. J. A **52**, 130 (2016).
[27] S.-I. Ando, Phys. Rev. C **97**, 014604 (2018).
[28] S.-I. Ando, J. Korean Phys. Soc. **73**, 1452 (2018).
[29] T. Teichmann, Phys. Rev. **83**, 141 (1951).
[30] S. R. Beane and M. J. Savage, Nucl. Phys. A **694**, 511 (2001).
[31] S.-i. Ando and C. H. Hyun, Phys. Rev. C **72**, 014008 (2005).
[32] S.-i. Ando, J. W. Shin, C. H. Hyun, and S.-W. Hong, Phys. Rev. C **76**, 064001 (2007).
[33] S.-I. Ando, Eur. Phys. J. A **33**, 185 (2007).
[34] E. Ryberg, C. Forssén, H.-W. Hammer, and L. Platter, Phys. Rev. C **89**, 014325 (2014).
[35] S.-I. Ando and C. H. Hyun, Phys. Rev. C **86**, 024002 (2012).
[36] T. Fuchs, J. Gegelia, G. Japaridze, and S. Scherer, Phys. Rev. D **68**, 056005 (2003).
[37] S.-i. Ando and H. W. Fearing, Phys. Rev. D **75**, 014025 (2007).
[38] D. Baye and E. M. Tursunov, J. Phys. G: Nucl. Part. Phys. **45**, 085102 (2018).
[39] P. Descouvemont and D. Baye, Phys. Lett. B **127**, 286 (1983).
[40] P. Descouvemont and D. Baye, Nucl. Phys. A **459**, 374 (1986).
[41] P. Descouvemont and D. Baye, Phys. Rev. C **36**, 1249 (1987).
[42] D. Foreman-Mackey *et al.*, Publ. Astron. Soc. Pac. **125**, 306 (2013).
[43] P. Tischhauser *et al.*, Phys. Rev. C **79**, 055803 (2009).
[44] P. Dyer and C. Barnes, Nucl. Phys. A **233**, 495 (1974).
[45] A. Redder *et al.*, Nucl. Phys. A **462**, 385 (1987).
[46] J. M. L. Ouellet *et al.*, Phys. Rev. C **54**, 1982 (1996).
[47] G. Roters *et al.*, Eur. Phys. J. A **6**, 451 (1999).
[48] L. Gialanella *et al.*, Eur. Phys. J. A **11**, 357 (2001).
[49] R. Kunz, M. Jaeger, A. Mayer, J.W. Hammer, G. Staudt, S. Harissopulos, and T. Paradellis, Phys. Rev. Lett. **86**, 3244 (2001).
[50] M. Fey, Ph.D. thesis, Universitat Stuttgart, 2004.
[51] H. Makii *et al.*, Phys. Rev. C **80**, 065802 (2009).
[52] R. Plag, R. Reifarth, M. Heil, F. Kappeler, G. Rupp, F. Voss, and K. Wisshak, Phys. Rev. C **86**, 015805 (2012).
[53] X. D. Tang *et al.*, Phys. Rev. C **81**, 045809 (2010).
[54] D. Schurmann *et al.*, Phys. Lett. B **711**, 35 (2012).
[55] N. Oulebsir *et al.*, Phys. Rev. C **85**, 035804 (2012).